An integrated optimal estimation approach to Spitzer Space Telescope focal plane survey

David S. Bayard*, Bryan H. Kang, Paul B. Brugarolas and D. Boussalis

Jet Propulsion Laboratory, 4800 Oak Grove Drive, Pasadena, CA, 91109, USA

ABSTRACT

This paper discusses an accurate and efficient method for focal plane survey that was used for the Spitzer Space Telescope. The approach is based on using a high-order 37-state Instrument Pointing Frame (IPF) Kalman filter that combines both engineering parameters and science parameters into a single filter formulation. In this approach, engineering parameters such as pointing alignments, thermomechanical drift and gyro drifts are estimated along with science parameters such as plate scales and optical distortions. This integrated approach has many advantages compared to estimating the engineering and science parameters separately. The resulting focal plane survey approach is applicable to a diverse range of science instruments such as imaging cameras, spectroscopy slits, and scanning-type arrays alike. The paper will summarize results from applying the IPF Kalman filter to calibrating the Spitzer Space Telescope focal plane, containing the MIPS, IRAC, and the IRS science instrument arrays.

Keywords: Spitzer Space Telescope, SIRTF, calibration, focal plane survey, optimal estimation

1. INTRODUCTION

This paper discusses the focal plane survey of the Spitzer Space Telescope. The approach taken for focal plane survey is novel in the sense that it is based on using a high-order 37-state Kalman filter that combines both engineering parameters and science parameters into a single filter formulation. In this integrated approach, engineering parameters such as pointing alignments, thermomechanical drift and gyro drifts are estimated along with science parameters such as plate scales and optical distortions.

The high-order estimator is denoted as the Instrument Pointing Frame (IPF) Kalman filter.[1–3] This integrated approach to the problem has the advantage of being able to correct engineering and science errors without issues of interference discussed in Ref. 4, and without requiring iteration between separate teams of engineering and science analysts. The IPF Kalman filter has been adopted by the Spitzer mission as the main calibration approach to support all focal plane survey efforts, and is the baseline method for providing frame calibration updates to the on-board frame table. Because of its high order, the Kalman filter had to be designed carefully using special scalings, a modern array square-root filtering approach, and advanced numerical techniques. The resulting focal plane survey approach is very general, and is applicable to a diverse range of science instruments such as imaging cameras, spectroscopy slits, and scanning-type arrays alike. An overview of the IPF Kalman filter design can be found in Refs. 1, 2 and complete algorithmic details in Ref. 3.

The paper will discuss results obtained from running the IPF Kalman filter on 76 different calibration data sets. These survey data sets are broken into Pre-Coarse, Coarse and Fine surveys. Due to space limitations, only results for the Fine surveys will be discussed since they are the most recent and accurate. The data sets include focal plane survey data for all of Spitzers's science instruments, i.e., MIPS, IRAC, and the IRS (both Peakup Arrays and Spectroscopy slits). The IPF filter supported updating 128 instrument pointing frames in the in-flight frame table, and over 1500 focal plane parameters characterizing alignments, plate scales, and optical distortions. This paper provides only a brief summary of the material covered in the focal plane survey final report in Ref. 5.

An overview of the calibration process in terms of the telescope focal plane, experiment design, and mission calibration timeline is given in Section 2. The focal plane parametrization is treated in more detail in Section 3. The main results of the paper are given in Section 4 which provides a top level summary of the focal plane survey, and a comparison with pre-flight accuracy predictions. Finally, in Section 5, a specific example is given highlighting the Fine Survey for the MIPS 24 um array. Conclusions are postponed until Section 6.

*david.bayard@jpl.nasa.gov; MS 198-326; phone (818) 354-8208; fax (818) 393-4440

2. OVERVIEW

2.1. Telescope Focal Plane

The telescope focal plane is shown in Figure 2.1 projected on the sky, as viewed by an observer who is located inside the celestial sphere. The 19 Prime frames are depicted, each of which is calibrated with a dedicated focal plane survey effort. Also shown are the Brown angle conventions, which are used for reporting all calibrated frame locations. The Brown angles correspond to a 3,2,1 Euler angle sequence, but with a nonstandard sign convention adopted by R.J. Brown.[6]

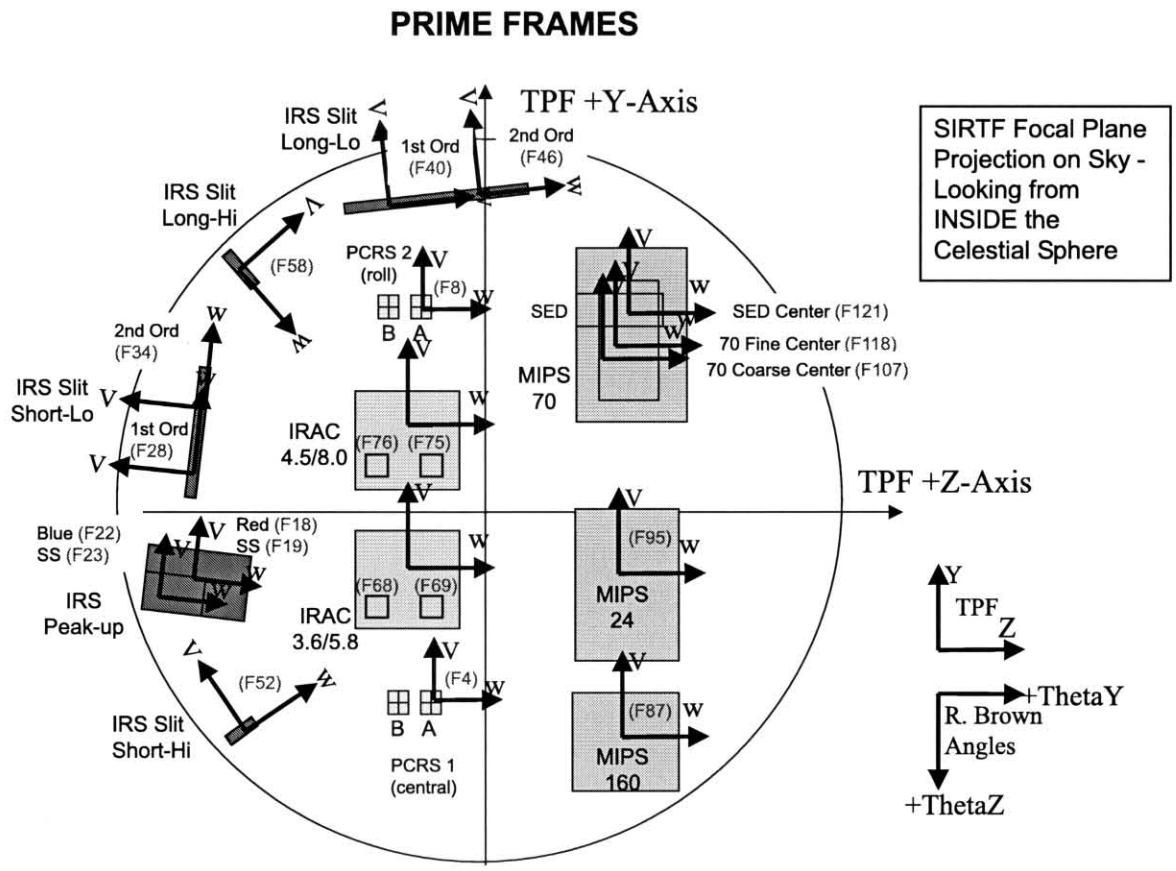

Figure 2.1. Prime frames in focal plane

2.2. Experiment Design Procedure

The calibration of the focal plane is performed using a series of experiments denoted as "Sandwich" maneuvers. A generic sandwich maneuver is shown in Figure 2.2 and consists of the following sequence of steps.

1. Locate a target star on the first Pointing Control Reference Sensor (PCRS) detector, PCRS 1, and take one or more centroid measurements.
2. Move the target star to PCRS 2, and take one or more centroid measurements
3. Move the target star to several positions on the desired science instrument array, and take a centroid measurement at each location (for example, a 3x3 grid pattern)
4. Return to the PCRS 1 detector, and take one or more centroid measurements.

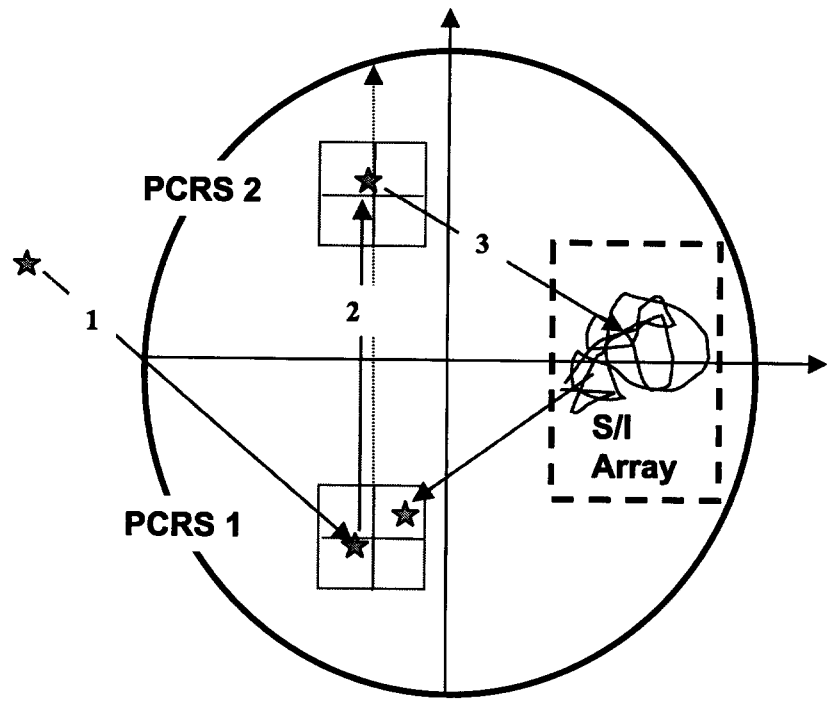

Figure 2.2. Sandwich maneuver for calibration experiment design

The centroids taken on the science array are arbitrary, but must result in a time-tagged list of centroids (with both x and y coordinates). This approach is very general, allowing for grid patterns, dither patterns, simultaneous star clusters, etc. For the MIPS instrument, the time-tagged list of centroids includes additional information about the size of the commanded scan mirror offsets, so that the scan mirror can be calibrated with respect to scale factor and alignment (i.e,. along track and cross-track type errors). For IRS spectroscopy slits, the centroids are "faked" in the sense that the source is scanned across the slit and the centroid is reported as being at the slit center at the time instant of maximum flux.

The Telescope Pointing Frame (TPF) is defined by the telescope boresight as referenced with respect to the location of the two PCRS boresight unit vectors. By transitioning between the two PCRS and the science array, the sandwich maneuver is informative about the location of the instrument pointing frame (IPF) with respect to the TPF (i.e., the alignment matrix T in Figure 3.1), and the TPF with respect to the body frame (i.e., the alignment matrix R in Figure 3.1). Also, by beginning and ending on the same PCRS, the sandwich maneuver is informative about accumulated attitude error due to gyro drift, which can be calibrated out accordingly. The sandwich maneuvers are repeated a statistical number of times to ensure that the random errors can be adequately reduced by smoothing the data.

2.3. Mission Calibration Timeline

A complete chronological listing of all official Spitzer focal plane survey calibration runs is depicted in Figure 2.3. For electronic displays of this paper, IRAC runs are shown in blue, IRS runs in red, and MIPS runs in green. A solid box indicates calibration runs that were used to update the on-board frame table. Dashed boxes indicate runs that were delivered to the mission archive, but were used primarily for diagnostic and comparison purposes.

Run labels have the form XXXYYY where XXX denotes the run number, and YYY denotes the frame table number of the associated Prime frame (a number from 1 to 128). Pre-Coarse surveys have run numbers containing the letter "P"; Coarse surveys have run numbers less than 500; and Fine surveys have run numbers greater than 500. It is seen that the surveys progressed from Pre-Coarse, to Coarse, to Fine, over the mission calibration period.

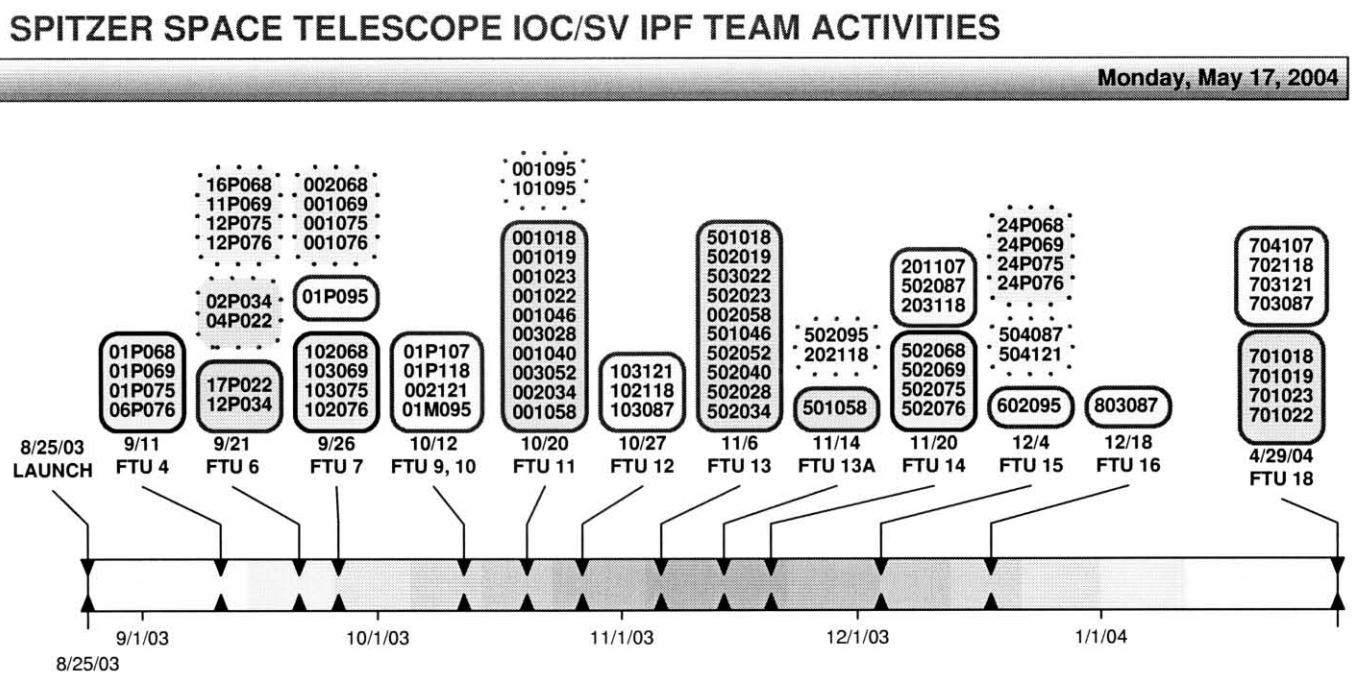

Figure 2.3. Mission timeline of all calibration runs

3. FOCAL PLANE PARAMETRIZATION

3.1. Pointing-Relevant Frames

The main frames relevant to the Spitzer's pointing system are shown in Figure 3.1. Here the focal plane is shown projected on the sky, as viewed by an observer who is located inside the celestial sphere. The key transformations between these frames are summarized in Table 3.1. For simplicity in presentation, the transformations A, R, T, C will denote 3×3 direction cosine matrices. (This is in contrast to the software implementation which uses quaternions for all numerical computations).

Transformation	Description	From	To
A	Attitude	ICRS	Body
R	Alignment	Body	TPF
T	Instrument	TPF	IPF_0
C	Scan Mirror Offset	IPF_0	IPF_Γ

Table 3.1. IPF Filter Transformations

The International Celestial Reference System (ICRS) frame serves as the Spitzer's principle inertial reference frame. With a suitable relabelling, the star-tracker instrument frame serves as the Spitzer's Body frame (i.e., when spelled with its boresight as the x axis[3]). The mapping from ICRS to the Body Frame is denoted as the spacecraft attitude A. During each sandwich maneuver, only gyro propagated attitude solutions are used by the IPF filter to reconstruct attitude. The current attitude A is attained from a gyro propagated offset G relative to a starting attitude A_0, i.e.,

$$A = GA_0 \tag{3.1}$$

where A_0 is available from the on-board attitude estimate. The Telescope Pointing Frame (TPF) has the telescope boresight as its x axis, and is defined rigorously in terms of the null points of the two PCRS sensors.[3] Specifically, the TPF is defined by a fixed (3,2,1) Euler rotation from the line-of-centers frame (constructed by bisecting and crossing the two PCRS boresight vectors). The mapping from the Body Frame to the TPF is denoted as the

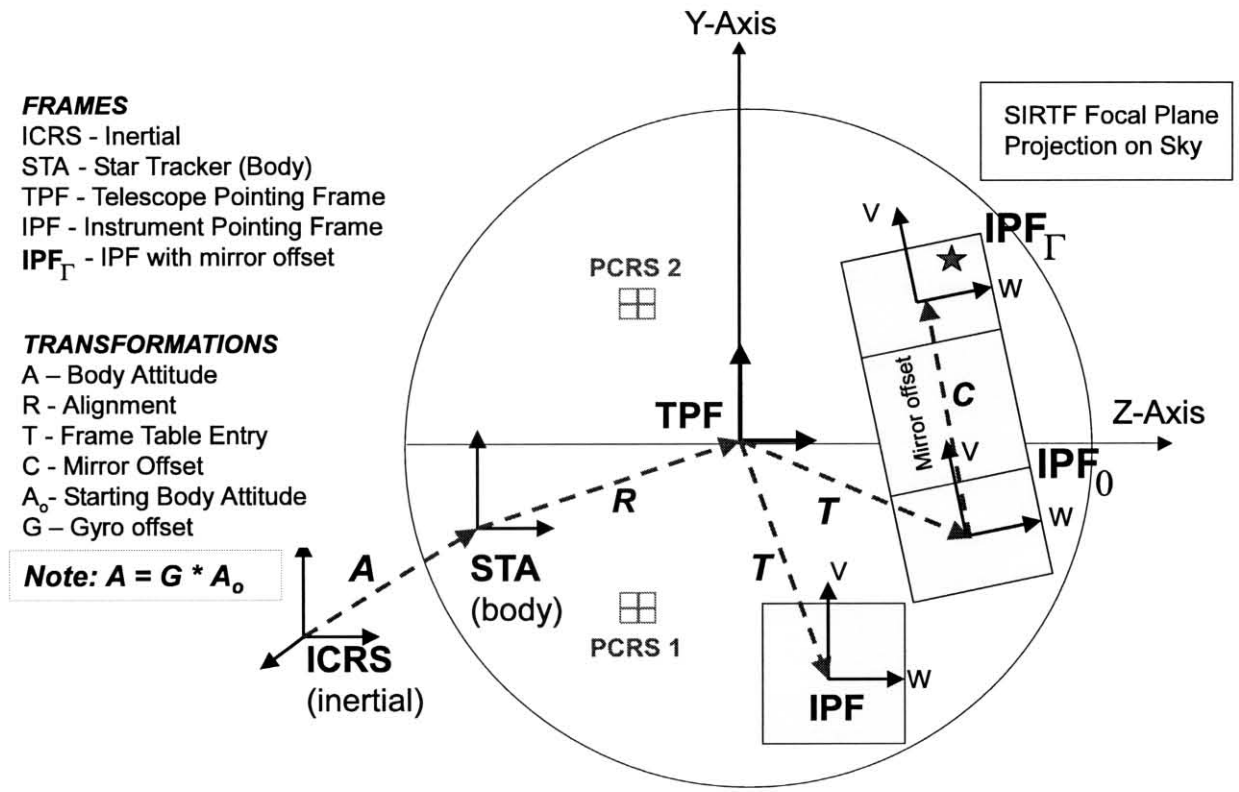

Figure 3.1. Spitzer Space Telescope frames and transformations

alignment matrix R.

An Instrument Pointing Frame (IPF) is defined by a specified pixel location within each science array, such that its coordinate axes adopt the orientation of the corresponding pixel rows and columns of that array. The mapping from the TPF to any specified IPF is denoted generically as T. Best estimates of the IPF frames are stored in an on-board "Frame Table" as 128 values for T (stored as quaternions). The Frame Table is used extensively for commanding purposes. Certain important IPF frames are denoted as **Prime Frames** (typically defined at the center pixel location of each instrument array). Other frames are called **Inferred Frames** and are defined by a pixel offset relative to a nearby Prime frame. The nominal orientations of the science instruments and their associated Prime frames in the telescope focal plane have been shown earlier in Figure 2.1. Also shown in Figure 2.1 are the mission-accepted conventions for the w and v directions, defined for each frame. Specifically, each IPF frame is defined by the u, v, w coordinate axes, where v, w are shown and $u = v \times w$ points outward to the sky. *The main goal of the IPF Kalman filter (as relevant to supporting on-board pointing capability) is to accurately estimate the IPF frame T for each of the 128 Prime and Inferred frames listed in the on-board Frame Table.* An important secondary goal is to provide plate scales and optical distortion parameters needed for correcting in-flight centroiding when using the IRS Peakup arrays. Other goals include supplying calibration parameters for ground pointing reconstruction efforts.

The C matrix represents a scan mirror offset from a nominal starting position $\Gamma = 0$ to its current local offset position $\Gamma \neq 0$. For non-MIPS instruments, the C matrix is set to identity. For MIPS, the frame defined when the scan mirror is offset by angle Γ is denoted as IPF_Γ. Note that as the scan mirror moves there is an entire family of IPF_Γ frames generated as a continuous function of the variable Γ.

The attitude A is time-varying due to intentional telescope repositioning and unintentional control errors. The alignment matrix R is time-varying due to thermo-mechanically induced alignment drift. The mapping T from TPF to IPF is assumed constant due to the fact that the telescope focal plane is actively cooled. The mapping C is time-varying due to a constantly changing (but nominally known) scan-mirror offset angle Γ.

3.2. Calibration Parameters

The calibration parameters are broken into two sets, p_1 and p_2. The p_1 set is made up of 17 science parameters, and the p_2 set is made up of 20 engineering parameters. The parameters in p_1 and p_2 are defined such that they are constant with time. Using a masking method, the IPF Kalman filter can estimate all 37 of these parameters or any subset, depending on what is best for the array being calibrated. The p_1 and p_2 parameters are given as follows:

$p_1(1:3) = \{a_{00}, b_{00}, c_{00}\}$ - Constant plate scales (i.e., the first-order term in a Taylor expansion)

$p_1(4:7) = \{a_{10}, b_{10}, c_{10}, d_{10}\}$ - Γ Dependent Plate Scales (i.e., constant plate scales scaled by the scan mirror offset Γ)

$p_1(8:11) = \{a_{20}, b_{20}, c_{20}, d_{20}\}$ - Γ^2 Dependent Plate Scales (i.e., constant plate scales scaled by the squared scan mirror offset Γ^2)

$p_1(12:17) = \{a_{01}, b_{01}, c_{01}, d_{01}, e_{01}, f_{01}\}$ - Linear Plate Scales (i.e., the second-order term in a Taylor expansion)

$p_2(1) = \alpha$ - Mirror misalignment (acts in cross-scan direction)

$p_2(2) = \beta$ - Mirror scale factor (acts in along-scan direction)

$p_2(3:5) = \{\theta_1, \theta_2, \theta_3\}$ - IPF frame (i.e., the three degrees of freedom associated with T)

$p_2(6:8) = \{a_{rx}, a_{ry}, a_{rz}\}$ - Tracker to TPF alignment (i.e., 3 degrees of freedom for the initial R)

$p_2(9:11) = \{b_{rx}, b_{ry}, b_{rz}\}$ - Tracker to TPF linear alignment (i.e., linear changes in R in time)

$p_2(12:14) = \{c_{rx}, c_{ry}, c_{rz}\}$ - Tracker to TPF quadratic alignment (i.e., quadratic changes in R in time)

$p_2(15:17) = \{b_{gx}, b_{gy}, b_{gz}\}$ - Gyro bias

$p_2(18:20) = \{c_{gx}, b_{gy}, c_{gz}\}$ - Gyro bias drift

4. TOP LEVEL SUMMARY

In total, the IPF Kalman filter was used to process 76 separate calibration data sets over the period of IOC/SV and Post-IOC. This consisted of 19 Pre-Coarse survey runs, 29 Coarse survey runs, and 28 Fine survey runs. Approximately 4 hours of mission time was allocated to each IPF Kalman filter run, as measured from the time the complete data set became available, to the time the calibration products were delivered to the mission archive. Based on these runs, approximately 1500 calibration parameters were estimated associated with frame alignments, pointing systematic errors, plate scales and optical distortions. The typical calibration accuracy goal was 5 arcseconds for the Pre-Coarse surveys, and 1 arcsecond for the Coarse surveys. The Fine surveys had the tightest requirements which are summarized in the next sections.

4.1. Focal Plane Survey Results

The calibration accuracy for each of the 19 Prime frames is summarized in Table 4.1, in units of arcseconds, 1-sigma, radial. The last column is denoted as "REQ", and lists the requirements as provided in Ref. 7. The second column from the right is denoted as "ACTL", and lists the actual calibration errors. By comparing these last two columns, it is seen that all of the main focal plane survey requirements are met.

The column marked "PRED" gives the predicted accuracies based on the pre-flight covariance analysis found in Ref. 8. Comparing this column with the "ACTL" column gives a comparison of how well the actual focal plane survey performed relative to the expected results. In general these two columns agree reasonably well.

A large improvement was seen in the IRAC 3.6 and 5.8 um array centers (frames 068, 069), where a 36 percent margin was achieved compared to a predicted 3 percent margin. This improvement can be attributed to a change in the experiment design by the IRAC team from a five-of-diamonds pattern to a "simultaneous star cluster" calibration set. The latter design contains significantly more centroids on the science array.

			BROWN ANGLE			ESTIM. ACCURACY		
			[amin]	[amin]	[deg]	[asec] 1σ radial		
NF	RN	DESCRIPTION	theta_Y	theta_Z	angle	PRED	ACTL	REQ
018	701	IRS_Red_PeakUp_FOV_Center	-11.649	2.000	1.797	0.1279	0.0899	0.25
019	701	IRS_Red_PeakUp_FOV_Sweet_Spot	-11.587	1.971	1.978	0.1009	0.0866	0.14
022	701	IRS_Blue_PeakUp_FOV_Center	-13.520	1.897	1.704	0.1285	0.0966	0.25
023	701	IRS_Blue_PeakUp_FOV_Sweet_Spot	-13.578	1.864	1.817	0.1014	0.0869	0.14
028	502	IRS_ShortLo_1st_Ord_Center_Pos	-12.033	-2.793	-84.720	0.1056	0.1165	0.14
034	502	IRS_ShortLo_2nd_Ord_Center_Pos	-11.913	-4.093	-84.720	0.1061	0.0909	0.14
040	502	IRS_LongLo_1st_Ord_Center_Pos	-4.406	-13.997	-1.200	0.2571	0.1295	0.28
046	501	IRS_LongLo_2nd_Ord_Center_Pos	-1.213	-14.066	-1.200	0.2587	0.2682	0.28
052	502	IRS_ShortHi_Center_Position	-10.565	10.010	-41.470	0.1037	0.0885	0.14
058	501	IRS_LongHi_Center_Position	-10.418	-10.232	43.340	0.1864	0.1027	0.28
068	502	IRAC_Center_of_3.6umArray	-2.860	3.737	-0.542	0.1358	0.0881	0.14
069	502	IRAC_Center_of_5.8umArray	-2.843	3.607	-0.301	0.1359	0.0889	0.14
075	502	IRAC_Center_of_4.5umArray	-2.721	-3.049	-0.720	0.1103	0.0878	0.14
076	502	IRAC_Center_of_8.0umArray	-2.752	-3.068	0.017	0.1103	0.0895	0.14
087	703	MIPS_160um_center_large_FOV	6.711	11.987	0.814	0.2413	1.2056	3.70
095	602	MIPS_24um_center	6.716	4.246	0.638	0.1235	0.0884	0.14
107	704	MIPS_70um_center	6.550	-8.069	-2.862	0.2957	0.2847	2.60
118	702	MIPS_70um_fine_center	7.126	-6.809	-8.474	0.2117	0.3038	1.10
121	703	MIPS_SED_center	6.056	-9.431	0.062	0.6392	0.9998	1.10

Table 4.1. Top Level Performance Summary (Predicted, Actual and Required)

The MIPS 160 um (frame 087) had much less margin than predicted from pre-flight analysis. The main reason is the use of a Seyfert galaxy as the calibration source, which had significant positional uncertainty (approx 1 arcsec) compared to other sources typically used for calibration (approx 0.1 arcsec). This 1" error mapped directly into the final frame calibration error.

The MIPS instrument experienced some unexpected challenges during the survey effort. The 70 micron arrays (wide and narrow) and SED suffered from significant centroiding degradation over half of the array; the 160 um suffered from stray-light problems; and the 24 um array suffered from a lack of scan-mirror repeatability on the order of 1". The stray light problem for the 160 um array was mitigated by using a Seyfert galaxy as the source. The bad centroiding seen in the 70 um arrays and SED were avoided by concentrating centroids only on the good side of the arrays. Because of scan mirror non-repeatability, Prime frame 095 and its inferred frames were ultimately derived by the MIPS team, based on averaging results from runs 502095 and 602095, which should be accurate to 0.5 arcseconds.

4.2. Comparison to Pre-Flight Estimates

Prior knowledge about the Spitzer telescope focal plane was available from ground-based optical performance tests made in the Brutus chamber at Ball Aerospace.[9,10] This provided the best alignment information for each of the Prime and Inferred frames prior to launch.

It is of interest to summarize the total amount of correction needed for each Prime Frame relative to this initial knowledge. This information is depicted graphically in Figure 4.1 and is summarized numerically in Table 4.2. The numerical values in Table 4.2 show the initial pre-launch alignments on the left (from `BodyFrames_FTU_00c`), the latest calibrated alignments in the middle (from `BodyFrames_FTU_18a`), and their difference on the right. These difference values are plotted as quivers in Figure 4.1, where they have been magnified by a factor of five to aid visualization.

Typical corrections were on the order of 0.1 to 0.2 arcminutes (i.e., 6-12 arcseconds). However, a large correction of 2 arcminutes was needed for the MIPS SED (frame 118), and other large corrections were needed for the other MIPS arrays. These large corrections could be traced to a large initial uncertainty in the MIPS scan mirror parameters, acting primarily in Theta_Y direction.

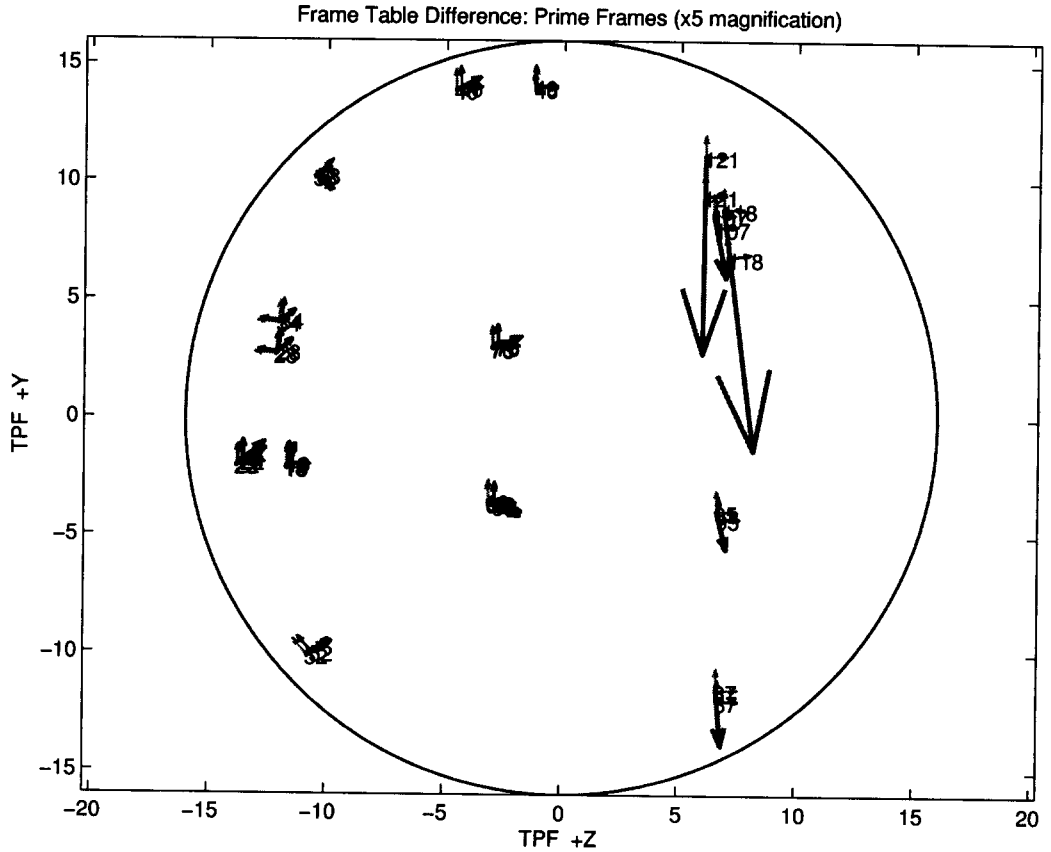

Figure 4.1. Alignment correction relative to pre-flight knowledge (quivers magnified 5 times)

NF	FTU 0			FTU18			DIFF: FTU18 - FTU0		
	BROWN ANGLE			BROWN ANGLE			BROWN ANGLE		
	Theta X	Theta Y	Theta Z	Theta X	Theta Y	Theta Z	Theta X	Theta Y	Theta Z
	[amin]	[amin]	[deg]	[amin]	[amin]	[deg]	[amin]	[amin]	[deg]
18	-11.7080	2.1380	2.9600	-11.6492	2.0004	1.7966	0.0588	-0.1376	-1.1634
19	-11.6496	2.1709	2.9600	-11.5870	1.9713	1.9779	0.0626	-0.1996	-0.9821
22	-13.7500	2.0370	2.9600	-13.5203	1.8967	1.7044	0.2297	-0.1403	-1.2556
23	-13.8114	2.0640	2.9600	-13.5784	1.8644	1.8172	0.2330	-0.1996	-1.1428
28	-12.1660	-2.6690	275.2800	-12.0326	-2.7926	275.2800	0.1334	-0.1236	0.0000
34	-12.0450	-3.9910	275.2800	-11.9131	-4.0932	275.2800	0.1319	-0.1022	0.0000
40	-4.6060	-13.8890	358.8000	-4.4057	-13.9970	358.8000	0.2003	-0.1080	0.0000
46	-1.1980	-13.9600	358.8000	-1.2134	-14.0662	358.8000	-0.0154	-0.1062	0.0000
52	-10.7640	10.1330	318.5300	-10.5647	10.0097	318.5300	0.1993	-0.1233	0.0000
58	-10.5440	-10.1580	43.3400	-10.4177	-10.2319	43.3400	0.1263	-0.0739	0.0000
68	-3.1240	3.6340	0.0000	-2.8605	3.7375	359.4577	0.2635	0.1035	359.4577
69	-3.1170	3.5160	0.0000	-2.8433	3.6067	359.6989	0.2737	0.0907	359.6989
75	-2.9600	-2.9500	0.0000	-2.7206	-3.0487	359.2799	0.2394	-0.0987	359.2799
76	-2.9800	-2.9910	0.0000	-2.7518	-3.0679	0.0171	0.2282	-0.0769	0.0171
87	6.6690	11.5170	0.0000	6.7110	11.9874	0.8143	0.0420	0.4704	0.8143
95	6.6410	3.9310	0.0000	6.7221	4.2538	0.6319	0.0811	0.3228	0.6319
107	6.4450	-8.5920	0.0000	6.5504	-8.0689	357.1381	0.1054	0.5231	357.1381
118	6.8590	-8.8470	0.0000	7.1226	-6.8087	351.5257	0.2636	2.0383	351.5257
121	6.0730	-11.0980	0.0000	6.0563	-9.4312	0.0620	-0.0167	1.6668	0.0620

Table 4.2. FTU 0 to FTU 18 Brown Angles

5. EXAMPLE: MIPS 24 UM ARRAY (FRAME 095)

In this section, the focal plane survey of the MIPS 24 um array (Fine survey run 602095) is highlighted in more detail. The experiment design is shown in Figure 5.1. Three measurements are taken at every PCRS location, and the pattern on the science array is a 7 by 3 grid of observations. Here, each row of 3 grid points is associated with a different sandwich maneuver. At each position in each row, the spacecraft attitude is fixed, and there are six scan mirror offsets moving the source 3 positions up and 3 positions down in approximately 25 arcsecond increments (some of which fall off the array and are not recorded).

The experiment design in Figure 5.1 is repeated twice for a total of 14 sandwich maneuvers, containing 460 science centroids and 126 PCRS measurements. The IPF filter estimates 33 parameters consisting of: 3 constant and 6 linear plate scales, 4 Gamma Dependent parameters, 2 mirror parameters, 3 IPF alignment angles, 3 STA-to-PCRS alignment angles, 6 STA-to-PCRS thermomechanical drift parameters, and 3 gyro bias and 3 gyro bias-drift parameters.

The nominal pixel size for the MIPS 24 um array is 2.4932 arcsecs (W direction), and 2.5981 arcsecs (V direction). To compare before and after results, the a-priori prediction errors are shown in Figure 5.2 with a size of 2.4059" RMS, radial, while the a-posteriori prediction errors are shown in Figure 5.3 with an improved size of 0.1785" RMS, radial. The quivers are magnified by 10 to aid visualization. The posterior error is essentially due to centroiding, indicating that the MIPS team achieved a centroiding accuracy error better than 1/14 pixel.

Results show remaining constant plate scale errors on the order of 1 part in a thousand, and significant high order optical distortions. The scan mirror has approximately a 4 percent scale factor error and a .7 degree misaligment with respect to the orientation of the 24 um array.

The optical distortions estimated by the IPF Kalman filter (at zero scan mirror offset) are plotted in the quiver plot Figure 5.4. As a comparison, the optical distortions obtained using a purely physical modeling approach (i.e., a Code V program) are shown in Figure 5.5. It can be seen that the quiver directions and sizes are in excellent agreement. This provides a cross-validation between the physical-based optical modeling, with the measurement-based IPF calibration results.

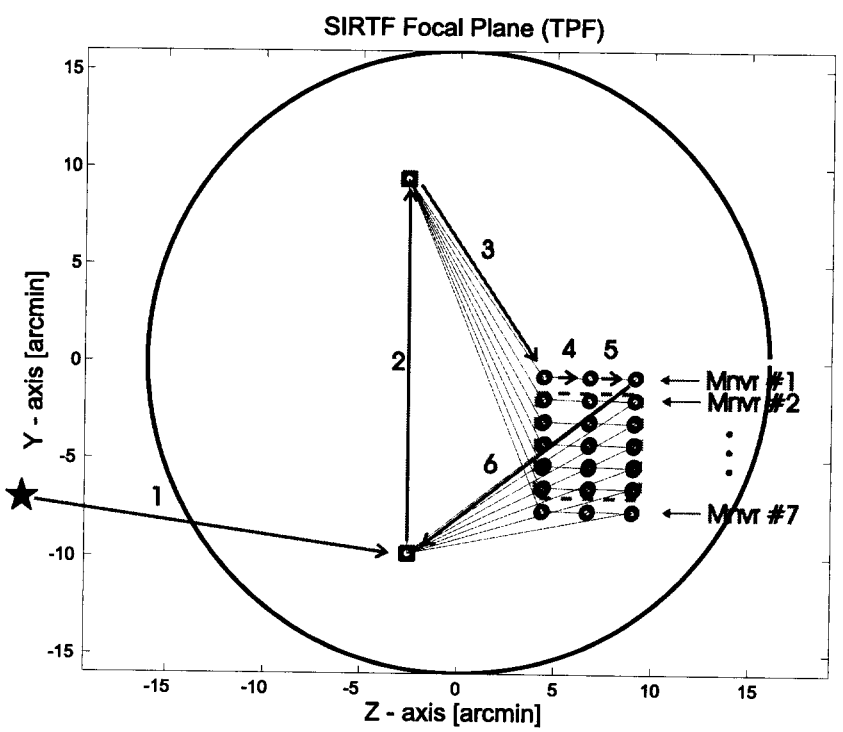

Figure 5.1. Experiment design for MIPS 24 um Array [ID602095]

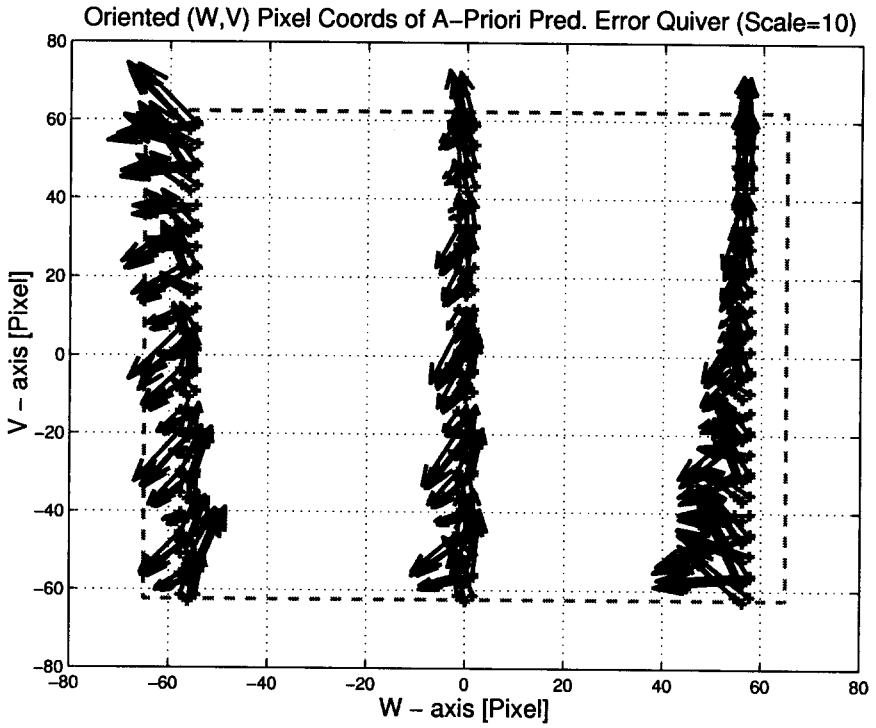

Figure 5.2. Oriented (W,V) Pixel Coords of A-priori prediction error quiver plot [RUN602095]

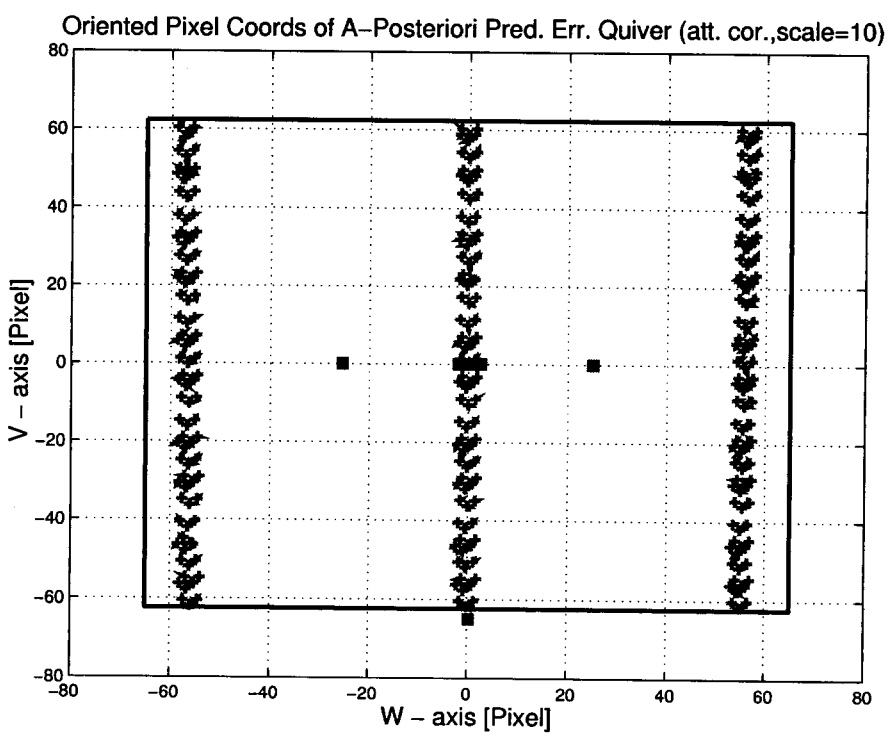

Figure 5.3. A-posteriori science centroid prediction error quiver (att. cor.) [RUN602095]

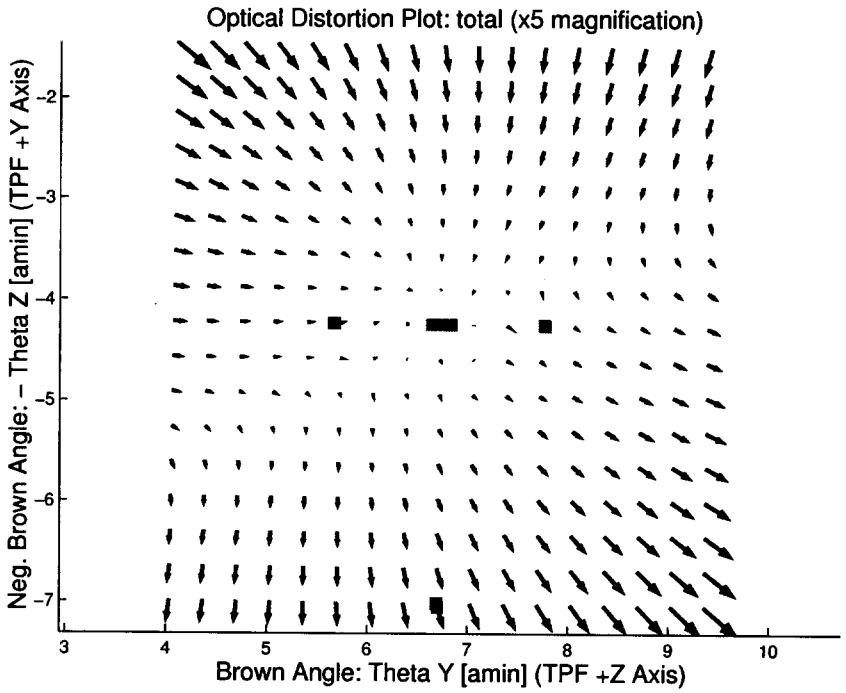

Figure 5.4. Optical distortion plot: total (x5 magnification) [RUN602095]

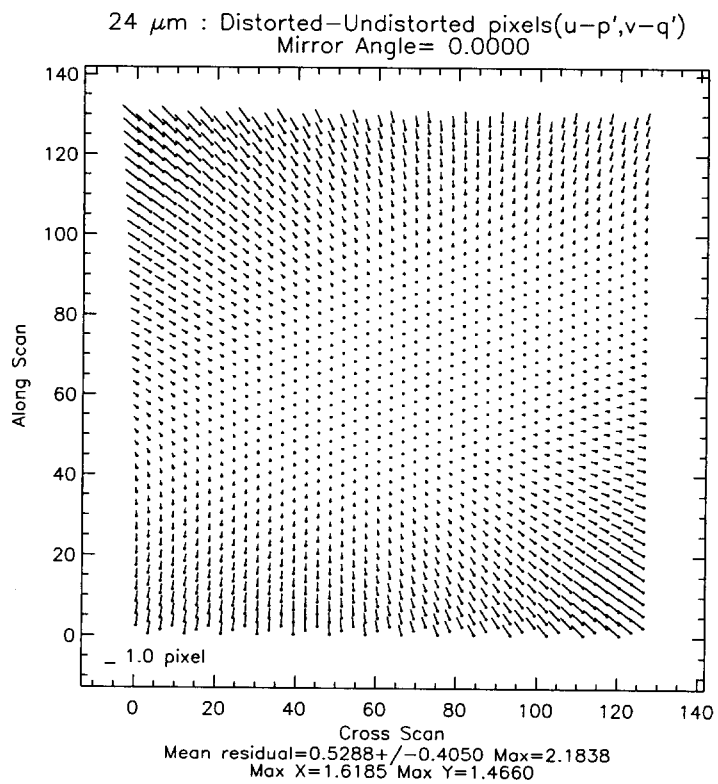

Figure 5.5. Optical distortion plot based on Code V (courtesy of Jane Morrison, Univ. of Arizona)

6. CONCLUSIONS

This paper summarizes an error analysis of the final focal plane calibration accuracies for the Spitzer Space Telescope. The main conclusion is that all focal plane calibration requirements have been met with the survey strategy as implemented. Margins range from 4 percent for the IRS Long-Lo slit, to 89 percent for the MIPS 70 um array. These results closely match pre-flight predictions of expected focal survey accuracies.

An unexpected event was the discovery of a 1 arcsecond non-repeatability in the MIPS scan mirror. This mostly impacts the MIPS 24 um array since the other MIPS arrays have greatly relaxed requirements.

For pointing purposes, the most critical calibrations are for the IRS Peakup sweet spots and short wavelength slit centers (frames 019, 023, 052, 028, 034). Results show that the these frames are meeting their 0.14" requirements with an expected accuracy of approximately 0.09", which corresponds to a 36 percent margin.

ACKNOWLEDGMENTS

This work was performed at the Jet Propulsion Laboratory, California Institute of Technology, under contract with the National Aeronautics and Space Administration. The focal plane survey required a highly collaborative effort involving a great many people across the entire Spitzer team (e.g., science, engineering, and mission operations) to whom we are very grateful. Due to space limitations, we list only our primary interfaces: Jocelyn Keene, Bill Wheaton, Jane Morrison (MIPS), Peter Eisenhardt, Sean Carey (IRAC), Carl Grillmair, Keven Uchida, Bernhard Brandl (IRS), Elmain Martinez, Myche McAuley (MIPL), Amy Mainzer (PCRS), Dan Swanson, Chris Voth, Dave Eckart, Angus McMechen (OET, Lockheed-Martin), John Gilbert, John Miles (IOC/SV planning), Keyur Patel, Bob Wilson (flight system), Fernando Tolivar, Tooraj Kia, Johnny Kwok, Mike Werner, Charles Lawrence, Nick Gautier, Jeff Van Cleve, and Bill Mahoney (consultations and advice).

REFERENCES

1. D.S. Bayard and B.H. Kang, *An Overview of the SIRTF Instrument Pointing Frame (IPF) Kalman filter for Focal Plane Calibration.* Jet Propulsion Laboratory, JPL Internal Document D-26417, December 9, 2003.
2. D.S. Bayard and B.H. Kang, "A high-order Kalman filter for focal plane calibration of NASA's Space Infrared Telescope Facility (SIRTF)," AIAA Guidance, Navigation and Control Conference and Exhibit, Paper # AIAA-2003-5824, Austin, TX, August 11-14, 2003.
3. D.S. Bayard and B.H. Kang, *SIRTF Instrument Pointing Frame (IPF) Kalman Filter Algorithm*, JPL Internal Document D-24809, September 30, 2003.
4. M.D. Shuster and R.V.F. Lopes, "Parameter interference in distortion and alignment calibration, AAS Paper AAS 94-186, Feb. 1994.
5. D.S. Bayard, B.H. Kang, P.B. Brugarolas and D. Boussalis, *Spitzer Space Telescope Focal Plane Survey Final Report*, JPL Internal Document D-27667, May 14, 2004; (includes Appendix A: IRS, D-27667A; Appendix B: IRAC, D-27667B; Appendix C: MIPS, D-27667C).
6. R.J. Brown, *Focal Surface to Object Space Field of View Conversion.* Systems Engineering Report SER No. S20447-OPT-051, Ball Aerospace & Technologies Corp., November 23, 1999.
7. *Space Infrared Telescope Facility In-Orbit Checkout and Science Verification Mission Plan*, JPL Internal Document D-22622, 674-FE-301 Version 1.4, February 8, 2002.
8. D.S. Bayard, P.B. Brugarolas, D. Boussalis, and B.H. Kang, *SIRTF Focal Plane Survey: A Pre-Flight Error Analysis.* JPL Internal Document D-26678, September 1, 2003; (includes Appendix A: IRS, D-26678A; Appendix B: IRAC, D-26678B; Appendix C: MIPS, D-26678C).
9. J.P. Schwenker, B.R. Brandl, W. Burmester, J. Hora, A.K. Mainzer, P.C. Quigley, J. Van Cleve, "SIRTF-CTA optical performance test," IR Space Telescopes and Instruments. Edited by John C. Mather. Proceedings of the SPIE, Volume 4850. pp. 304-317, 2003.
10. J.P. Schwenker, B.R. Brandl, W.F. Hoffman, J. Hora, A.K. Mainzer, J.E. Mentzell, J. Van Cleve, "SIRTF-CTA optical performance test results," IR Space Telescopes and Instruments. Edited by John C. Mather. Proceedings of the SPIE, Volume 4850. pp. 30-41, 2003.